Structural, Optical and Electrical Properties of Spray Pyrolysis Deposited CdS Films

Shashikant D. Gunjal,[1,4] *Yogesh B. Khollam*,[2] *Sandeep A. Arote*,[1] *Sandesh R. Jadkar*,[1] *Pandit N. Shelke*,[3] *Kakasaheb C. Mohite**[1,4]

Summary: The n-type cadmium sulfide (CdS) is one of the most promising materials for hetero-junction thin film solar cell applications due to its wide bandgap (2.42 eV). In present communication, the deposition of pure CdS films with hexagonal symmetry by using home-built spray pyrolysis technique and aqueous solutions of $CdCl_2$ and $NH_2.CS.NH_2$ as the precursor materials is reported. The films were deposited at the substrate temperatures of 200, 250 and 300 °C with UHP nitrogen as a carrier gas and characterized by using X-ray diffraction (XRD), UV-visible spectroscopy and Hall Effect measurement. The structural studies by using XRD showed that the resultant films have strong orientation of CdS crystallites along (101) with hexagonal structure (wurtzite type). The average crystallite size is found to be 17 nm. The UV-visible spectroscopy studies of resultant films showed the optical transmittance equal to ≈50% and bandgap is found to be between 2.39 – 2.41 eV. The resistivity and average Hall coefficient are found to be 1.451×10^1 cm and - 1.557×10^3 cm^3/C respectively. The resultant films are observed to be good to make a solar cell with CdS as a window layer.

Keywords: CdS films; electrical properties; optical properties; spray pyrolysis; X-ray

Introduction

Cadmium sulfide (CdS) an inorganic group II-VI semiconductor compound is easy to isolate and purify. It is the promising material for hetero-junction thin film solar cell devices and a principal source of cadmium for all commercial applications. The wide bandgap (2.42 eV) CdS is now become a well known n-type partner as a 'window layer' with p-type semiconductor such as CdTe, Cu_2S, InP and $CuInSe_2$ in hetero-junction thin film solar cell devices.[1–2] CdS forms the core component of a photovoltaic solar cell on combining with a p-type semiconductor. The light penetrates through the transparent CdS window layer and then absorbed in p-type semiconductor at the junction.[3] A hetero-junction CdS/Cu_2S was one of the first efficient solar cells reported in 1954 and now CdS is usually used an n-type partner for CdS/CdTe hetero-junction solar cell.[4] The current reports of National Renewable Energy Laboratory (NREL), USA show the highest efficiency of 20.4% for hetero-junction CdS/CdTe solar cell. In other applications, CdS is used in photoresistors, in thin-film transistors (TFTs) and as a pigment material.[5] Different physico-chemical techniques like closed space sublimation[3–8],chemical bath deposition[9–13], pulsed laser deposition[14–16], spray pyrolysis[1,17–19], electrochemical deposition[20], dip-coating process[21–22], metal organic chemical vapors deposition (MOCVD)[23] and thermal evaporation[24] are reported in

[1] School of Energy Studies, Department of Physics, University of Pune, Pune 411 007, India
[2] Department of Physics, Anantrao Pawar College, Pirangut, Pune 412 115, India
[3] Department of Physics, Baburaoji Gholap College, Sangvi, Pune 411 027, India
[4] Department of Physics, H. V. Desai College, Pune 411 002, India
E-mail: kcmohite@gmail.com

literature to deposit CdS thin films. The chemical spray pyrolysis is the most suitable method to deposit II-VI semiconductor materials for scientific as well as industrial applications. In view this, the present communication deals with the preparation of single phase CdS films by using the home-built spray pyrolysis deposition technique. The physical, optical and electrical characteristics of as-prepared CdS films are presented in present paper.

Experimental Part

In present work, $CdCl_2.H_2O$ and $NH_2.CS.NH_2$ (thiourea) were used as precursor materials to deposit CdS films by using home-built spray pyrolysis technique on thoroughly cleaned soda lime glass (SLG) substrates. Initially, 0.1 M solutions of $CdCl_2.H_2O$ and $NH_2.CS.NH_2$ were prepared in double distilled water (DDW) separately. These two solutions were mixed together ultrasonically for 30 min. with continuous stirring. The SLG substrates were cleaned thoroughly by using the procedure as given in following steps: (1) washing with laboline detergent & then rinsing with DDW, (2) heating in concentrated chromic acid (0.5 M) for 1 hr & then keeping in it for 12 hr, (3) cleaning ultrasonically in DDW and (4) finally, cleaning in AR grade acetone for 10 min. Before the deposition of films, the spray chamber was purged with ultra high pure (UHP) nitrogen gas for 15 min. Further, the nitrogen gas was also used as a carrier gas to spray the final precursor solution on preheated SLG substrates. The films were deposited on thoroughly cleaned SLG substrates at different substrate temperatures of 200, 250 and 300 °C by using the following processing parameters: (i) spray gun nozzle to substrate distance = 22 cm, (ii) concentration of spray solution = 0.1 M, (iii) carrier N_2 gas flow rate = 15 lpm, (iv) deposition time = 10 min., and (v) solution flow rate = 5 ml/min. After the deposition, the films were cooled naturally to the room temperature (RT). The X-ray diffraction (XRD) patterns of resultant films were recorded by using the using X-ray diffractrometer (Bruker D8 Advance machine, Germany) with CuKα radiation (λ = 1.5418 Å) in 2θ range of $20 - 80^0$. The XRD patterns were used for structural analysis of different films. The values of thickness of resultant films were obtained by using the KLA Tencor P_16+ surface profilometer. The UV-Visible transmission spectra were recorded by using JASCO Model: V670 spectrometer and used to estimate optical properties: transmission (% T) and band gap (E_g) of resultant films. The electrical properties: sheet & bulk charge carrier concentrations (n), mobility (μ), resistivity (ρ), conductivity (σ) and Hall coefficient (R_H) were obtained by using Hall measurement set-up (ECOPIA HMS-3000) at room temperature with current = 10 nA and magnetic field = 0.54 Tesla.

Results and Discussion

X-Ray Diffraction (XRD)

Figure 1 gives the X-ray diffraction (XRD) patterns of resultant films prepared by using home-built spray pyrolysis deposition technique at different substrate temperatures of 200, 250 and 300 °C.

By using the Bragg's diffraction condition;

$$2d\sin\theta = n\lambda \quad (1)$$

[where, d = interplanar spacing, θ = angle of diffraction, n = order of diffraction and λ = 1.54 Å (wavelength of X-rays)], the d values are calculated for different planes of all the XRD patterns. The observed 'd' values are found to be very close to the standard data given in PCPDF data file No. 41–1049 for hexagonal CdS phase. However, in case of the XRD pattern of a film deposited at lower substrate temperature of 200 °C, the additional reflections corresponding to the cubic CdS [PCPDF file no.: 21– 0829] and CdO [PCPDF file no.: 21– 0829] phases are also observed. Further, in case of the XRD pattern of a film deposited at substrate temperature of

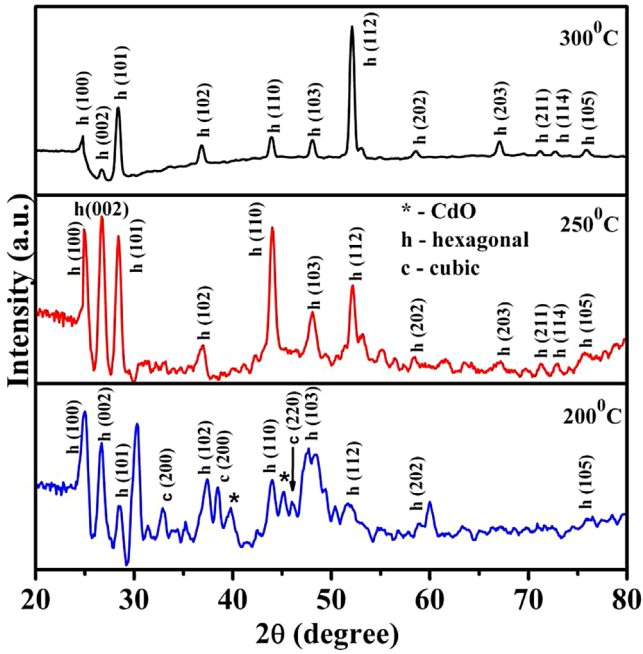

Figure 1.
XRD patterns of the films deposited at different substrate temperatures of 200, 250 and 300 °C.

250 °C, the reflections corresponding to the cubic CdS [PCPDF file no.: 21–0829] phase having very low intensities are also seen. This indicates the formation of CdS films with mixed phase at lower substrate temperatures of 200 and 250 °C. Thus, the films deposited at substrate temperature of 300 °C indicate the formation of single CdS phase with hexagonal symmetry in resultant films.

The Bragg's diffraction condition [equation (1)] and d-spacing relation for hexagonal symmetry;

$$\frac{1}{d^2} = \frac{4}{3}\left(\frac{h^2 + hk + k^2}{a^2}\right) + \frac{l^2}{c^2} \qquad (2)$$

are used to obtain the values of lattice parameters: a and c for different resultant films. The calculated values of lattice parameters: a and c for resultant films deposited at different substrate temperatures (T_s) are given Table 1. It is observed that, the calculated values of 'a' and 'c' are found to be perfectly matching with standard values: a = 4.1409 Å and c = 6.7198 Å respectively given in PCPDF data file no.: 41–1049 for hexagonal CdS phase. The texture coefficient (TC) and standard deviation (σ_g) of the resultant films are calculated by using the following equations (3) and (4) respectively.[7–8] This study gives the understanding of growth mechanism of CdS films with respect to substrate temperature.

$$TC(hkl) = \frac{I(hkl)/I_0(hkl)}{\frac{1}{N}\sum_N I(hkl)/I_0(hkl)} \qquad (3)$$

$$\sigma_g = \frac{1}{N}\left[\sum_N (TC(hkl))^2 - 1\right]^{1/2} \qquad (4)$$

Table 1 gives the data for texture coefficient (TC) and standard deviation (σ_g) obtained from (101) planes only for the films deposited at substrate temperatures of 250 and 300 °C. For both the films deposited at substrate temperatures of 250 and 300 °C, the values of TC are found to be

Table 1.
Data for TC, σ_g and lattice parameters for films deposited at different substrate temperatures.

Substrate temperature (T_s), °C	(hkl) plane	TC	σ_g	d (Å)	a (Å)	c (Å)
200	--	--	--	--	--	--
250	101	0.74	0.34	3.1390	4.0987	6.6716
300	101	0.34	0.57	3.1391	4.1989	6.6818

highest for the (101) planes. Hence, the data for texture coefficient (TC) and standard deviation (σ_g) indicates the preferred orientation along (101) direction for both the films deposited at substrate temperatures of 250 and 300 °C.

The crystallite size (d) was calculated by using Scherrer formula[17–18]

$$d = \frac{0.9\lambda}{\beta\cos\theta} \quad (5)$$

where, d = crystallite size, λ = wavelength of X- rays, β = angular line width at the half - maximum intensity (FWHM) and θ = Bragg's diffraction angle. The (101) reflection is more symmetric without having any shoulders/satellite at higher as well as lower side of diffraction angle as compared to the other diffraction planes like (110), (112) etc. Hence, no base line correction is necessary for obtaining FWHM of (101) plane required for the calculation of crystallite size. Hence, the values of crystallite size are obtained from (101) plane. Table 2 gives the data for crystallite size of resultant films.

The values for the crystallite size are found to be in nanometric range. This clearly indicates the nano-crystalline nature of resultant films deposited at different substrate temperatures (T_s). The average crystallite size is found to be ~ 17 nm.

Surface Profilometer Studies

The thickness values of films deposited at different substrate temperature (T_S) of 200, 250 and 300 °C are found to be 1.00, 0.50 and 0.31 μm respectively. The thickness of film is found to be decreasing with increasing the substrate temperature from 200 to 300 °C. The films are prepared on thoroughly cleaned soda lime glass (SLG) substrates at different substrate temperatures of 200, 250 and 300 °C by using the following deposition parameters: (i) concentration of spray solution = 0.1 M, (iii) carrier N_2 gas flow rate = 15 lpm, (iv) deposition time = 10 min., and (v) solution flow rate = 5 ml/min. During the preparation of films at different substrate temperatures, same deposition parameters are used. After each deposition, all the films are cooled naturally to the room temperature (RT). Hence, decrease in film thickness observed with increasing the substrate temperature might be due to the densification of films at higher deposition temperature.

Optical Properties

Figure 2 shows the transmittance (% T) curves for the CdS films deposited at different substrate temperatures of 200, 250 and 300 °C. The average transmission for films deposited at different substrate temperatures is found to be nearly 50%. At

Table 2.
Data for the crystallite size for films deposited at different substrate temperatures.

Substrate temperature, (°C)	hkl plane	2θ (deg.)	FWHM β(θ)	FWHM β (radian)	d (nm)
200	(101)	28.4	0.5163	9.006×10^{-3}	15.87
250	(101)	28.4	0.5269	9.191×10^{-3}	15.55
300	(101)	28.4	0.4366	7.616×10^{-3}	18.77

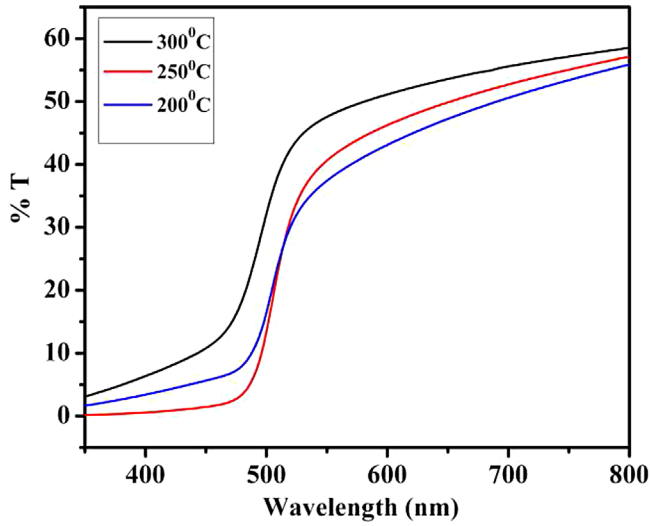

Figure 2.
Transmittance (% T) curves for films deposited at different substrate temperatures.

lower substrate temperature the film shows lower transmission. The % transmission is found to be increasing with increasing substrate temperature. This is might be due to the well crystallization of pure single phase of CdS at higher substrate temperature. It further indicates that, to obtain the highly transparent CdS layer, substrate temperature must be increased.

The values for optical band gap (E_g) are obtained from Tauc's plots generated by using the relation,

$$(\alpha h\nu)^2 = (h\nu - Eg) \tag{6}$$

Where, α = absorption coefficient, h = Planck's constant and ν = frequency. The absorption coefficient (α) is calculated by using the transmittance and thickness of the film given by equation (7).[1]

$$\alpha = -\left(\frac{2.303}{t}\right) log_{10}\left(\frac{1}{T}\right) \tag{7}$$

Where, t = thickness of film and T= % transmittance of the film.

Figure 3 gives the Tauc's plots for the films deposited at different substrate temperatures of 200, 250 and 300 °C. The extrapolation of straight-line portion of Tauc plot (intercept on X-axis) of a given film gives the value of band gap energy of corresponding film. The values of band gaps are found to be 2.39, 2.40 and 2.41 eV for the films deposited at the substrate temperature of 200, 250 and 300 °C respectively. This data is matching with the reported value of band gap for hexagonal CdS phase [20–24]. No significant change in the optical band gap is noted. This is might be due to increasing in the substrate temperature with a small step of ~ 50 °C. Due to increase in the substrate temperature with a small step of ~ 50 °C, there might be small change in the particle size (not given) leading to the no significant variation in the optical band gap.

Hall Measurement

From XRD analysis, the films deposited at substrate temperature of 300 °C only indicate the formation of single CdS phase with hexagonal symmetry in resultant films. Hence electrical properties are recorded for the films deposited at substrate temperature of 300 °C only. The electrical properties of the films deposited at substrate temperatures of 200 and 250 °C were not

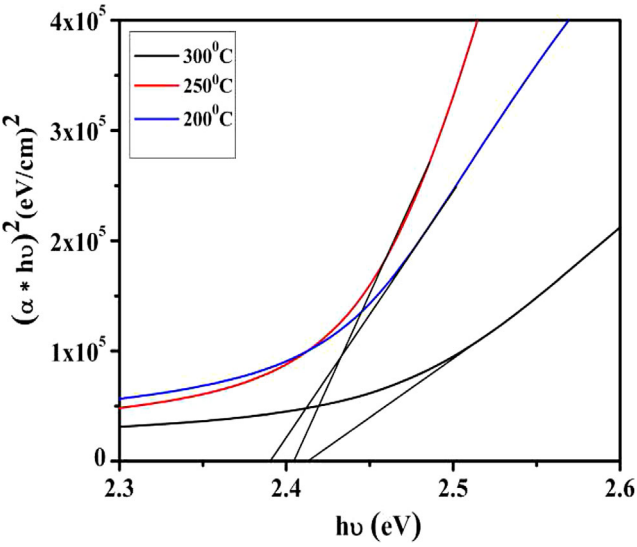

Figure 3.
Tauc's plot for the films deposited at different substrate temperatures.

recorded beacuse of their mixed phase nature. The electrical properties of the films deposited at substrate temperatures $= 300\ ^{\circ}C$ are found to be (i) sheet concentration of majority charge carriers $= -057.7 \times 10^{11}\ cm^{-2}$, (ii) bulk conconcentartion of majority charge carriers $= -8.242 \times 10^{15}\ cm^{-3}$, (iii) electrical resistivity $= 1.451 \times 10^{1}\ \Omega cm$, (iv) mobility $= 8.619 \times 10^{1}\ cm^2/Vs$ and (v) average Hall coefficient $= -1.557 \times 10^{3}\ cm^3/C$. The negative sign of Hall coefficient and the positive value of current observed in Hot probe experiment indicate n-type semiconducting nature of the resultant films. Further study to understand the experimental results obtained related to measurements of electrical properties of CdS films deposited at the substrate temperature of $300\ ^{\circ}C$ by using the Hall measurement set-up is in progress.

Conclusion

The spray pyrolysis is found to be cheap and easy in operation technique for the preparation of non-scratchable, well adherent and uniformly thick nano-crystalline CdS films. The films deposited at substrate temperature $(T_S) = 300\ ^{\circ}C$ are having single CdS phase with hexagonal symmetry. The thickness of film is found to be decreasing with increasing substrate temperature due to the densification of films. The average % transmittance is found to be increasing with increasing the T_S. This is might be due to the increasing crystallization with higher phase purity of films deposited at higher T_S. The average % transmittance is found to be ~ 50. The data obtained for the band gap values for different films is found to be matching with the reported values of band gap for hexagonal CdS phase. The measurement of Hall coefficient and hot probe experiment showed that the CdS films deposited at different T_S are having n-type semiconducting nature. Thus CdS films prepared in present work by using spray pyrolysis technique can be used as a window layer (n-type semiconductor) in hetero-junction solar cells applications.

Acknowledgements: Author SDG is thankful to BCUD, University of Pune for providing the financial support to present research work.

Author SDG is also grateful to Prof. S. V. Ghaisas, Director, School of Energy Studies, University of Pune for providing research facilities to present research work.

[1] R. K. Sharma, K. Jain, A. C. Rastogi, *Curr. Appl. Phys.*, **2003**, *3*, 199.
[2] A. Ashour, *Turk J. Phys.*, **2003**, *27*, 551.
[3] H. R. Moutinho, D. Albin, Y. Yan, R. G. Dhere, X. Li, C. Perkins, C.-S. Jiang, B. To, M. M. Al-Jassim, *Thin Solid Films*, **2003**, *436*, 175.
[4] H. Zhao, A. Farah, D. Morel, C. S. Ferekides, *Thin Solid Films*, **2009**, *517*, 2365.
[5] P. K. Weimar, *Proc. IRE*, **1962**, *50*, 1462.
[6] W. Mahmood, N. A. Shah, *AIP Conf. Proc.*, **2012**, *1476*, 178.
[7] C. Barret, T. B. Massalski, *"Structure of Metals"*, Pergamon, Oxford **1980**. p. 204.
[8] C. M. Mahajan, M. G. Takwale, *Curr. Appl. Phys.*, **2013**, *13*, 2109.
[9] J. Hiie, T. Dedova, V. Valdna, K. Muska, *Thin Solid Films*, **2006**, *511–512*, 443.
[10] O. Vigil-Galan, A. Morales-Acevedo, F. Cruz-Gandarilla, M. G. Jimenez-Escamilla, J. Aguilar-Hernandez, G. Contreras-Puente, J. Sastre-Hernandez, E. Sanchez-Meza, M. L. Ramon-Garcia, *Thin Solid Films*, **2007**, *515*, 6085.
[11] B. Pradhan, A. K. Sharmab, A. K. Ray, *J. Crys. Growth.*, **2007**, *304*, 388.
[12] M. E. Calixto, M. Tufino-Velazquez, G. Contreras-Puente, O. Vigil-Galan, M. Jimenez-Escamilla, R. Mendoza-Perez, J. Sastre-Hernandez, A. Morales-Acevedo, *Thin Solid Films*, **2008**, *516*, 7004.
[13] S. A. Vanalakar, S. S. Mali, R. C. Pawar, N. L. Tarwal, A. V. Moholkar, A. Jin, Y.- Kim, J. H. Kwon, P. S. Kim, Patil, *Electrochimica. Acta*, **2011**, *56*, 2762.
[14] G. Perna, V. Capozzi, M. Ambrico, V. Augelli, T. Ligonzo, A. Minafra, L. Schiavulli, M. Pallara, *Thin Solid Films*, **2004**, *454*, 187.
[15] X. L. Tong, D. S. Jiang, Z. M. Liu, M. Z. Luo, Y. Li, P. X. Lu, G. Yang, H. Long, *Thin Solid Films*, **2008**, *516*.
[16] N. Hernandez-Como, V. Martinez-Landeros, I. Mejia, F. S. Aguirre-Tostado, C. D. Nascimento, G. M. Azevedo, C. Krug, M. A. Quevedo-Lopez, *Thin Solid Films*, **2014**, *550*, 665.
[17] V. V. Ison, A. Ranga Rao, V. Dutta, D. K. Avasthi, *Nuc. Instr. Meth. Phys. Res. B.*, **2007**, *262*, 209.
[18] K. Ravichandran, P. Philominathan, *Solar Ener.*, **2008**, *82*, 1062.
[19] S. J. Ikhmayies, R. N. Ahmad-Bitar, *Appl. Surf. Sci.*, **2010**, *256*, 3541.
[20] O. A. Ileperuma, C. Vithana, K. Premaratne, S. N. Akuranthilaka, S. M. Mcgregor, I. M. Dharmadasa, *J. Mater. Sci.: Mater. In Electro.*, **1998**, *9*, 367.
[21] I. O. Oladejia, L. Chowa, J. R. Liub, W. K. Chub, A. N. P. Bustamantec, C. Fredricksena, A. F. Schultea, *Thin Solid Films*, **2000**, *359*, 154.
[22] P. P. Hankare, P. A. Chate, D. J. Sathe, *Solid State Sci.*, **2009**, *11*, 1226.
[23] K. S. Youn, K. H. Yu, J. S. Song, I. H. Choi, *J. Korean Physical Soc.*, **2005**, *47*, 89.
[24] Z. R. Khan, M. Zulfequar, M. S. Khan, *Mater. Sci. Engg. B.*, **2010**, *174*, 145.

